Fast-timing lifetime measurements of excited states in ^{67}Cu

C. R. Niţă,[1,2,*] D. Bucurescu,[1] N. Mărginean,[1] M. Avrigeanu,[1] G. Bocchi,[3,4] S. Bottoni,[3,4] A. Bracco,[3,4] A. M. Bruce,[5] G. Căta-Danil,[1] G. Coló,[3,4] D. Deleanu,[1] D. Filipescu,[1] D. G. Ghiţă,[1] T. Glodariu,[1] S. Leoni,[3,4] C. Mihai,[1] P. J. R. Mason,[6,7] R. Mărginean,[1] A. Negret,[1] D. Pantelică,[1] Z. Podolyak,[6] P. H. Regan,[6] T. Sava,[1] L. Stroe,[1] S. Toma,[1] C. A. Ur,[8] and E. Wilson[6]

[1]*Horia Hulubei National Institute of Physics and Nuclear Engineering (IFIN-HH), Bucharest 077125, Romania*
[2]*University Politehnica of Bucharest, Bucharest 060042, Romania*
[3]*Dipartimento di Fisica, University of Milano, Milano, Italy*
[4]*INFN, Sezione di Milano, Milano, Italy*
[5]*School of Computing, Engineering and Mathematics, University of Brighton, Brighton BN2 4GJ, UK*
[6]*Department of Physics, University of Surrey, Guildford GU2 7XH, UK*
[7]*STFC Daresbury Laboratory, Daresbury, Warrington WA4 4AD, UK*
[8]*INFN, Sezione di Padova, Padova, Italy*

(Received 16 September 2013; revised manuscript received 30 April 2014; published 25 June 2014)

The half-lives of the $9/2^+$, $13/2^+$, and $15/2^+$ yrast states in the neutron-rich ^{67}Cu nucleus were determined by using the in-beam fast-timing technique. The experimentally deduced E3 transition strength for the decay of the $9/2^+$ level to the $3/2^-$ ground state indicates that the wave function of this level might contain a collective component arising from the coupling of the odd proton $p_{3/2}$ with the 3^- state in ^{66}Ni. Theoretical interpretations of the $9/2^+$ state are presented within the particle-vibration weak-coupling scheme involving the unpaired proton and the 3^- state from ^{66}Ni and within shell-model calculations with a ^{56}Ni core using the jj44b residual interaction. The shell model also accounts reasonably well for the other measured electromagnetic transition probabilities.

DOI: 10.1103/PhysRevC.89.064314 PACS number(s): 29.30.Kv, 23.20.Lv, 21.10.Tg, 27.50.+e

I. INTRODUCTION

In the medium-mass region of nuclei with $Z \sim 28$ approaching the $N = 40$ subshell closure, it is assumed from empirical observations [1–3] and theoretical calculations [4] that states with different structures such as single-particle, intruder, and collective states coexist at low and medium excitation energies. The nature of the single-particle states in $_{27}$Co and $_{29}$Cu nuclei with even numbers of neutrons is defined, in a simplistic view, by the odd hole/particle excitations on the available shell-model orbits, while collective aspects of the negative-parity states $(3^-, 5^-, \dots)$ of the $^{A\pm1}_{28}$Ni cores may manifest themselves in the higher excited states [1,3]. In $A \leqslant 69$ odd-mass Cu isotopes, studies with direct one-proton transfer reactions (^{3}He,d), (d,^{3}He), (α,t), and (t,α) [5–9] systematically evidenced $3/2^-$ (g.s.), $1/2^-$, $5/2^-$, and $9/2^+$ states having important $p_{3/2}$, $p_{1/2}$, $f_{5/2}$, and $g_{9/2}$ single-particle components, respectively. For ^{67}Cu the same conclusion is supported by a study with the (α,p) direct reaction [10]. The excitation energy of the $9/2^+$ state remains approximately constant from ^{61}Cu to ^{71}Cu [11]. The $9/2^+$ state in ^{63,65}Cu was studied also by inelastic scattering of protons, and the deduced B(E3; $9/2^+ \rightarrow 3/2^-$) transition strength was found to be comparable to those of the 3^- states in the ^{62,64}Ni neighboring nuclei [12]. Thus, the $9/2^+$ excited states in the odd-A Cu isotopes appear to present both proton single-particle and collective components. In Ref. [3] the $9/2^+$ and the $15/2^+$ levels in ^{67}Cu were proposed to result from the coupling scenario $\pi(2p_{3/2}) \otimes 3^-,6^-$ (^{66}Ni), respectively. Therefore, the Cu nuclei represent a good choice to test whether both the single-particle and the collective characters of the decays can be reproduced by state-of-the-art calculations.

As a neutron-rich nucleus, ^{67}Cu can be reached by a limited number of reactions. A level scheme at low excitation energies and low and medium spins was built [13] based on β-decay [14] and direct transfer reactions such as (d,^{3}He) [7], (α,p) [10,15], and (t,p) [16]. The analysis of spectroscopic factors pointed out that both $3/2^-_{\text{g.s.}}$ and $9/2^+_1$ states have important single-particle $\pi(2p_{3/2})$ and $\pi(1g_{9/2})$ components, respectively [7,10]. Information on higher spin states was recently obtained by γ-ray spectroscopy in two deep-inelastic reaction studies [3,11]. The level scheme was extended and it was suggested that two of the states are isomeric [3]: the $9/2^+$ level at 2503 keV ($T_{1/2} < 0.3$ ns) and the $15/2^+$ level at 3463 keV ($0.6 < T_{1/2} < 2.4$ ns). The measured half-life limits for the 3463-keV state indicate a large hindrance of the 99.9-keV M1 transition. Of special interest is the observation of the fast and particularly strong E3 transition of 2503 keV from $9/2^+$ to the $3/2^-$ ground state.

The structure of the $9/2^+$ level is not expected to change dramatically when passing from ^{65}Cu to ^{67}Cu, however, the decay pattern of this state in ^{67}Cu is different compared to that in the lighter isotopes. The same behavior as in ^{67}Cu is observed for ^{69}Cu. The general tendency in odd-mass ^{59,61,63,65}Cu isotopes is that the $9/2^+$ level decays through several relatively intense E1 transitions [3,11]. It can be remarked that approaching $N = 40$ the decay pattern for the $9/2^+$ level becomes similar in both ^{67}Cu and ^{69}Cu. Moreover, the branching ratios of the E3 transitions in ^{59,65,69}Cu are similar, while in ^{67}Cu it is found to be an order of magnitude higher [11]. There is another premise which hints at a

*crnita@tandem.nipne.ro

different configuration that may imply a particle-core coupling component: if one considers a mean value among odd-even Cu isotopes with $N \leqslant 40$ of $B(\mathrm{E1}; 9/2^+ \rightarrow 7/2^-) \sim 10^{-5}$ W.u., then the $B(\mathrm{E3})$ value in ^{67}Cu should be much larger than 10 W.u. [3].

Concerning the structure of the $15/2^+$ state, the coupling scheme $\pi(2p_{3/2}) \otimes 6^-$ was proposed by Asai *et al.* [3]. The level scheme of ^{66}Ni was recently revised [17] and the initially suggested nanosecond-isomeric state 6^- was lowered in energy by 58 keV relative to the 5^- state, no experimental half-life value being available for the 6^- state at present.

We present the results of measurements aimed at determining the lifetimes of the $9/2^+$ and $15/2^+$ proposed isomeric states [3] of ^{67}Cu, using the electronic fast-timing technique [18–20]. These measurements also allowed the determination of the lifetime of the $13/2^+$ state at 3363.3 keV. The experimental setup and the results of the lifetime measurements are discussed in Secs. II and III, while in Sec. IV an attempt is made at a theoretical interpretation of the $9/2^+$ state within a particle-vibration coupling (PVC) model. Shell-model calculations performed in the $f_{5/2}p_{3/2}p_{1/2}g_{9/2}$ space are also presented in order to provide a microscopic description of the low-lying excited states and, in particular, of the $9/2^+$ state and its E3 decay to the ground state.

II. EXPERIMENT

The ^{67}Cu nuclei were produced in an α-induced reaction on a thick, highly enriched, and self-supported ^{64}Ni target at an incident energy of 18 MeV. The α beam was delivered by the 9-MV tandem accelerator at IFIN-HH and γ rays were detected using a setup which consisted of five HPGe detectors, four planar HPGe detectors, and eight $LaBr_3$(Ce) scintillation detectors. The array of scintillation detectors was composed of three detectors with 2×2–in. cylindrical crystals, three with 1.5×1.5–in. crystals, and two with conical 1×1.5–in. crystals.

The trigger condition was that at least two $LaBr_3$(Ce) and one HPGe or two HPGe detectors fired in coincidence. Under this condition the total number of recorded events was $\approx 5 \times 10^8$.

The most intense reaction channels were ^{64}Ni(α,n)^{67}Zn and ^{64}Ni(α,$2n$)^{66}Zn. The incident energy was chosen to maximize the production of ^{67}Cu in the (α,p) channel on the basis of the calculated cross section. The cross section for producing ^{66,67}Zn nuclei is an order of magnitude higher, and therefore the transitions belonging to ^{67}Cu are superimposed on the significant background of γ rays from the two aforementioned nuclei. At this incident energy of 18 MeV, levels of spin up to $17/2^+$ and 3988-keV excitation energy were observed in ^{67}Cu. A clean selection of the γ-ray transitions from the channel of interest was impossible using only the HPGe detectors, and therefore a gate onto the 99.9-keV transition de-exciting the $15/2^+$, 3463-keV level was made in the planar HPGe detectors.

The energy calibration and the alignment of the time signals were performed using standard ^{60}Co and ^{152}Eu sources. Run-by-run gain matching was performed in the off-line analysis. To sum up the time response contributions from all the HPGe and scintillation detectors it was necessary to calibrate and align the time signal and, further, to correct for the time walk induced by the CFD modules. The electronics employed in processing the time signals and the procedure is presented in detail in Ref. [20]. For this step, the full energy peaks of the 1173.2- and 1332.5-keV transitions from ^{60}Co were used. The measured time resolution of the $LaBr_3$(Ce) detectors with respect to one of the conical crystals is 220–370 ps, depending on the crystal size.

The mixed array of HPGe and fast scintillation detectors enabled the selection of the $17/2^+ \rightarrow 15/2^+ \rightarrow 13/2^+ \rightarrow 9/2^+ \rightarrow 3/2^-_{\mathrm{g.s.}}$ decay branch in ^{67}Cu and the negative-parity levels lying at an excitation energy lower than that of the $9/2^+_1$ level. A delayed time spectrum for a level was obtained by selecting the γ rays which populate and subsequently de-excite it. Using the GASPWARE software package, data were sorted into E_{γ_1}-E_{γ_2}-ΔT cubes using the gating condition on the 99.9-keV γ-ray in the LEP detectors, where E_{γ_1} and E_{γ_2} represent the energy selections made in the $LaBr_3$(Ce) detectors and ΔT is their time difference. For the background subtraction a similar cube was sorted with a selection on the background close to the 99.9-keV transition in the energy spectrum taken with the planar HPGe detectors. The experimental lifetimes were obtained from the time distributions ΔT with selected gates on the energy axes. For each contribution of the time distribution a peak and a background component were considered. The final time distribution was obtained after subtracting the corresponding background: first, from the planar HPGe gate and, second, from the "start"-"stop" selections using the $LaBr_3$(Ce) detectors.

As shown in the previous work in which ^{67}Cu was investigated [3,11], the 99.9-keV transition belongs unambiguously to this nucleus and depopulates the $15/2^+$ state. The relevant part of the level scheme for ^{67}Cu as proposed after the most

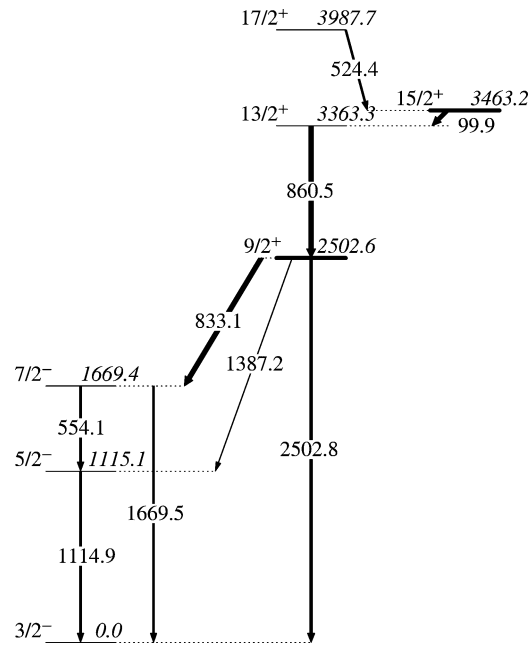

FIG. 1. Partial level scheme for ^{67}Cu reproduced after Ref. [11] (their Table IV) including only yrast levels observed in the present measurement.

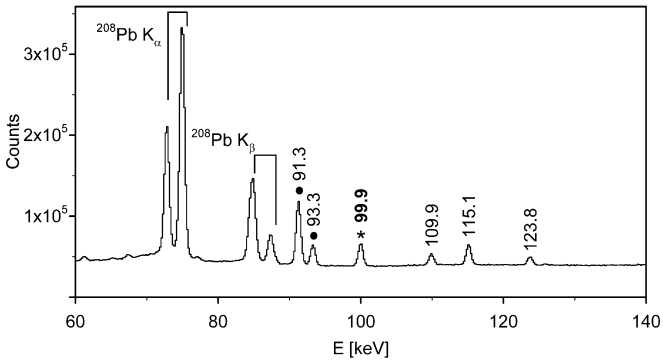

FIG. 2. Unconditioned γ energy spectrum from planar HPGe detectors measured following the reaction ^{64}Ni(α,p)^{67}Cu. The lead x rays appear due to the shieldings of the HPGe detectors. Lines marked with a black circle represent de-excitations of levels for ^{67}Zn, the 99.9-keV line for ^{67}Cu is marked with an asterisk, and the remaining γ lines belong to other residual nuclei or are from the activation of other Ni isotopes present in the target.

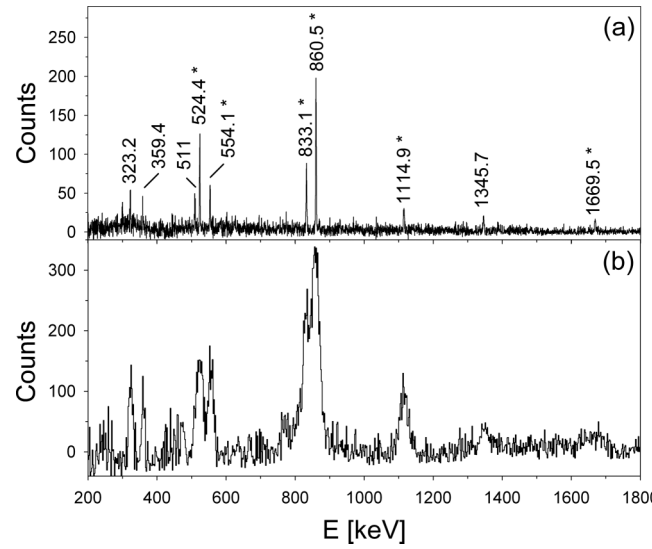

FIG. 3. Energy spectra acquired with the (a) HPGe and (b) $LaBr_3$(Ce) detectors, with a gate condition on the 99.9-keV transition in the planar HPGe detectors. All transitions marked with an asterisk belong to the ^{67}Cu nucleus.

extensive measurement performed with the Gammasphere array [11] is presented in Fig. 1. Figure 2 shows the quality of the selection for the full energy peak and the Compton background of the 99.9-keV transition, as well as the level of statistics.

III. EXPERIMENTAL RESULTS

In this section we present the experimental results of the half-life analysis for the $9/2^+$, $13/2^+$, and $15/2^+$ states of ^{67}Cu, obtained by fast-timing techniques with the $LaBr_3$(Ce) detectors [20]. As the starting point of the analysis, the prompt curve, giving the intrinsic time response of the system, was determined using γ rays originating from the strongest ^{67}Zn reaction channel. In particular, the 702.3- and the 814.6-keV transitions were considered, since they populate and depopulate the $7/2^-_1$ state with a known half-life of $2.0^{+1.4}_{-0.7}$ ps [13], well below the expected time resolution. The FWHM of the Gaussian-shaped time distribution was found to be 230 ps.

A. The half-life of the 2502.6-keV state

The 860.5-keV transition directly populates the 2502.8-keV level and was chosen as the "start" transition. This level is de-excited by the 833.1-, 1387.2-, and 2502.8-keV transitions. It is shown in Fig. 3 that, gating on the 99.9-keV line the 860.5- and 833.1-keV transitions are clearly identified, and an 860-833-ΔT cube was sorted as explained in the previous section. Because of the background included in the gate on the planar HPGe and implicitly in the E_{γ_1}-E_{γ_2}-ΔT cube sorted afterwards, choosing only the 860/833-keV combination did not provide sufficient statistics. The level of statistics was increased by including several other contributions to the time distributions, as explained below. The B(E2; $J^- \rightarrow 3/2^-$) strengths for the $J = 7/2$ and $5/2$ levels were determined in a COULEX experiment [2], and from these values the derived half-lives of the two states are of the order of a few picoseconds. These values are much lower than the time resolution of our experimental setup, and consequently all γ transitions that de-excite the levels below the $9/2^+$ level can be considered as prompt.

The final time distribution of this state, presented in Fig. 4, comprises the contributions of the 833.1-, 554.1-, 1114.9-, and 1669.5-keV transitions as "stop" transitions. For each "start"-"stop" pair of transitions a bidimensional banana-type selection was made both for the peak and for the corresponding background in the $LaBr_3$:Ce E_{γ_1}-E_{γ_2} matrix (see also Ref. [20]), thus determining background-corrected contributions, which were added up to provide the final time distribution. The background contribution to the time

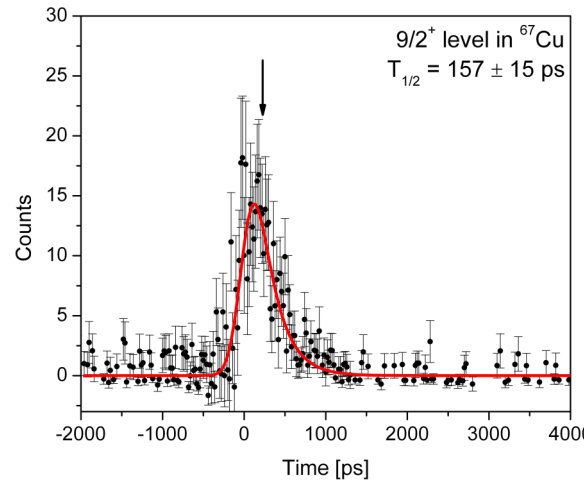

FIG. 4. (Color online) Time distribution for the $9/2^+$ state. The half-life was obtained with the convolution method. The solid line represents the fit with a function of the type exponential decay folded with the apparatus response function. The centroid of the time distribution, also used to determine the half-life by the centroid shift method (see text), is marked with an arrow.

distribution turned out to be a prompt distribution. The half-life has been obtained by fitting the final time distribution with an exponential decay folded with the prompt response function of the detection system. The experimental value was determined to be 157 ± 15 ps. Furthermore, a centroid shift analysis provides a half-life of 159 ± 37 ps, in very good agreement with the previous value.

In order to determine transition probabilities for the decays from the $9/2^+$ state, their branching ratios are needed. After using the 99.9-keV gating condition on the LEP detectors in order to emphasize the weak (α,p) reaction channel, our statistics did not allow accurate determination of these branching ratios. There are two sets of such branching ratios in the literature: those adopted by ENSDF [13] on the basis of the work of Asai *et al.* [3] and those recently published by Chiara *et al.* [11]. The branching ratios for the 833.1-, 1387.2-, and 2502.8-keV transitions from the $9/2^+$ state are (as a percentage) 58.3(24), 6.3(18), and 35.5(16) in Ref. [11] and 47(5), 6.1(19), and 47(7) in Ref. [3], respectively, thus showing discrepancies of about 20% for the 833.1-keV transition and 30% for the 2502.8-keV transition. For our analysis, we have chosen to use the values provided by the experiment with better statistics by Chiara *et al.* [11]. With these branching ratios and our lifetime, one obtains the following reduced transition probabilities. The 2502.8-keV transition has $B(\mathrm{E3};\ 9/2^+ \rightarrow 3/2^-) = 16.8 \pm 1.7$ W.u. For the 833.1-keV transition (assuming a pure E1) and 1387.2-keV transition one obtains $B(\mathrm{E1}) = (0.264 \pm 0.027) \times 10^{-5}$ W.u. and $B(\mathrm{M2}) = 0.146 \pm 0.015$ W.u., respectively. The B(E1) strength is about one order of magnitude smaller than the typical values from the lighter isotopes, contrary to the assumption in Ref. [3] [similarity of B(E1) values along the Cu isotopic chain]. For ^{69}Cu it is known experimentally that the $9/2^+$ state undergoes an E1 transition to the $7/2^-$ state at 1870.8 keV [21], but there is no present knowledge of the lifetime of this state [22]. A study of the E1 decays from the $9/2^+$ state would require a much larger shell-model space, including both the $f_{7/2}$ and the $g_{9/2}$ orbits, which is outside the purpose of the present investigation.

B. The half-lives of the 3463.2- and 3363.3-keV states

A similar procedure was employed for the 3363- and 3463-keV levels. The $15/2^+$ state decays only by the 99.9-keV M1 transition to the $13/2^+$ state, which in turn decays by the 860.5-keV transition. However, the 99.9-keV transition is not a suitable selection, as it was chosen as a gate in the planar HPGe detectors. Considering that the population of the 3463.2-keV state is smaller than that of the 2502.6-keV state and that the expected lifetime is of the order of nanoseconds [3], the 860.5-keV transition was selected as "stop," while for the "start" a wide gate was taken, comprising all γ rays in the energy range 520–1200 keV.

The 860.5-keV stop gate was chosen so as to avoid a contribution from the neighboring 833.1-keV transition (Fig. 3). Even if the latter transition still makes a small contribution, this does not change the conclusions of the analysis of the time distribution, as described below. The start gate includes the transition of 524.4 keV that directly feeds the 3463.2-keV level, as Fig. 1 indicates, and also the transitions due to the decay of the states below the 3463.2-keV state, namely, those of 554.1 keV ($7/2^- \rightarrow 5/2^-$), 1114.9 keV ($5/2^- \rightarrow 3/2^-$), 833.1 keV ($9/2^+ \rightarrow 7/2^-$), and 860.5 keV ($13/2^+ \rightarrow 9/2^+$). The lower energy limit was fixed so as to avoid the 511-keV annihilation contribution, which may include a delayed component in the final time distribution. Given that one of the gating selections covers a wide energy interval, an investigation of the Compton background from this gate is worthwhile. This was made by keeping the LEP 99.9-keV condition (and correcting for its background) and setting a gate on the 860.5-keV transition in the $LaBr_3$(Ce) detectors. In the resulting doubly gated $LaBr_3$(Ce) spectrum, only those transitions from ^{67}Cu that are known to be coincident with both the 99.9- and the 860.5-keV transitions remained. Therefore, the background from the start gate is largely due to the transitions that were considered as selections, with possible weak contributions from unobserved higher transitions feeding the $15/2^+$ state.

This triple coincidence analysis shows, for example, that the 1345.7-keV γ ray (shown in the spectra in Fig. 3) does not contribute to the time distribution.

The LEP selection of the 99.9-keV transition allowed us to access only the lifetime values of the $15/2^+$ (3463.2-keV) and the $13/2^+$ (3363.3-keV) states. This is a consequence of the unique decay path of the 3463.2-keV state, made only through the 99.9-keV transition. The $13/2^+$ state is fed only by the decay of the $15/2^+$ state. The theoretical time distribution of this two-level cascade decay is

$$f(t) = \frac{\tau_2}{\tau_1 - \tau_2}\left(e^{-\frac{t}{\tau_1}} - e^{-\frac{t}{\tau_2}}\right), \tag{1}$$

where τ denotes the lifetime, and indices 1 and 2 label the $15/2^+$ and $13/2^+$ states, respectively. This function starts from a zero value at $t = 0$, increases to a maximum at $t_M = \tau_1\tau_2 \ln(\tau_1/\tau_2)/(\tau_1 - \tau_2)$, and then decreases to 0. If τ_2 is very short compared to the experimental time resolution (that is, the 860.5-keV transition can be considered prompt), $f(t)$ practically reduces to the exponential decay of state 1 ($15/2^+$). Such a single-exponential fit to the right side of the time distribution from Fig. 5 is not suitable, especially as one cannot describe the region from 0 up to about 2 ns. Actually, this region shows a dip around 1 ns and a maximum at about 2 ns, suggesting the fact that the lifetime of the $13/2^+$ state (τ_2) is in the nanosecond range as well. This is also supported by the relative intensities of the 99.9- and 860.5-keV transitions reported in Ref. [3], which show that the 3363.3-keV state still survives after a 1.8-ns flight time of the ^{67}Cu nuclei. Therefore, the 0.6- to 2.4-ns half-life interval assigned to the $15/2^+$ state [3] actually refers to a combination of the lifetimes of both the $15/2^+$ and the $13/2^+$ states.

The experimental time distribution in Fig. 5 was fitted with a complex function which accounts for its two components. By imposing the wide start gate, the final time distribution includes a contribution given by the γ rays below the $15/2^+$ state that de-excite the $9/2^+$ state and the states lower in excitation energy, with half-lives lower than a few picoseconds. The shape of this component is identical to that in Fig. 4, but reversed in time. The second component, appearing as a tail

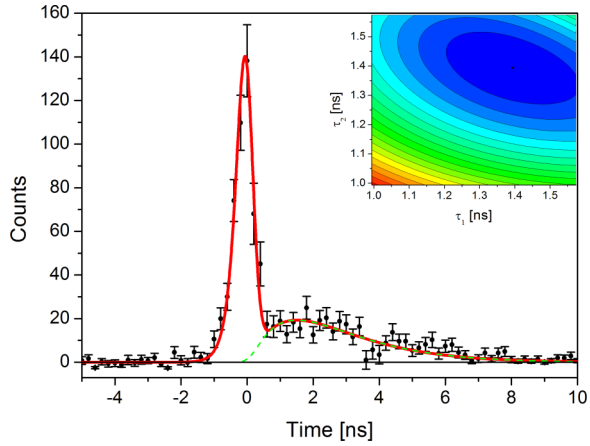

FIG. 5. (Color online) Time distribution corresponding to the decay of the $13/2^+$ state, as populated through the $15/2^+ \rightarrow 13/2^+ \rightarrow 9/2^+$ cascade. The solid (red) line represents the global fit of the distribution with a function considering the contributions of the lifetimes of the $9/2^+$, $13/2^+$, and $15/2^+$ states, as described in the text. The dashed (green) line shows the contribution due to the decay of the $15/2^+$ and $13/2^+$ states. Inset: Evolution of the χ^2 value of the fit as a function of the lifetimes of the two states, showing a minimum at $\tau_1 \simeq \tau_2$ (iso-χ^2 curves shown in steps of 0.2). The adopted lifetimes are $\tau_1 = \tau_2 = 1.39 \pm 0.18$ ns.

on the $t > 0$ side was described with the two-level formula, (1), folded with the (Gaussian) time response function of the detection system. The best fit, shown in Fig. 5, was obtained for quasi-equal $\tau_1 \simeq \tau_2 = 1.39 \pm 0.18$ ns, with τ_2 differing from τ_1 by about 0.01%. An inspection of the χ^2 surface in the τ_1 and τ_2 variables (inset in Fig. 5) also shows a minimum around $\tau_1 = \tau_2$. Therefore, we adopt, for both the $15/2^+$ and the $13/2^+$ states, half-lives of 0.96 ± 0.13 ns. For the $\tau_1 = \tau_2 = \tau$ case one can deduce an analytical formula which avoids the singularity of formula (1). A fit with this formula provided a value of τ consistent with the solution found with formula (1). With these lifetimes we obtain electromagnetic transition probabilities of $B(\mathrm{M1};\ 15/2^+ \rightarrow 13/2^+) = (2.18 \pm 0.29) \times 10^{-2}$ W.u. (assuming a pure M1 transition) and $B(\mathrm{E2};\ 13/2^+ \rightarrow 9/2^+) = 0.08 \pm 0.01$ W.u.

IV. THEORETICAL INTERPRETATION

A. Particle-vibration coupling-model calculations

An attempt has been made to interpret the $9/2^+$ state of ^{67}Cu by means of the particle-vibration weak-coupling model of Bohr and Mottelson [23,24]. The model, recently applied in Refs. [25] and [26] in connection with recent experiments on ^{47,49}Ca, describes excited states in odd nuclei arising upon coupling a phonon excitation of the even-even core nucleus with an unpaired particle/hole of the final system. In the case of ^{67}Cu, we have attempted to identify the $\pi(2p_{3/2}) \otimes 3^-$ multiplet, arising from the coupling of the octupole phonon of ^{66}Ni to the unpaired $p_{3/2}$ proton of ^{67}Cu, and, in particular, to calculate both the energies and the electromagnetic transition probabilities of its members.

TABLE I. Top: Energy and B(E3) values for the 3^- phonon of ^{66}Ni, as calculated by the QRPA model with SkX and SLy5 Skyrme forces. Experimentally, only the energy of the state is known. For comparison purposes, the footnote gives the corresponding experimental B(E3) strength in ^{64}Ni [30]. Bottom: Energy and B(E3) values for the $9/2^+$ state of ^{67}Cu, as obtained either experimentally or by means of the PVC model (see text for details).

		E (MeV)	B(E3) (W.u.)
3^-	Expt.	3.370	—[a]
	Theory		
	SkX	4.4	7.9
	Sly5	5.2	7.5
$9/2^+$	Expt.	2.503	16.8 ± 1.7
	Theory		
	SkX	2.9	5.4
	Sly5	2.9	5.2

[a] In ^{64}Ni, $B(\mathrm{E3}) = 10.83 \pm 0.59$ W.u. [30].

First, the properties of the 3^- phonon of ^{66}Ni have been obtained with microscopic HF-BCS plus QRPA calculations (cf. Ref [27] for details), employing two Skyrme parameter sets (SkX [28] and SLy5 [29]). For neutrons the usual zero-range, density-dependent pairing interaction

$$V_p(\vec{r}_1,\vec{r}_2) = V_0\left[1 + \eta\left(\frac{\rho((\vec{r}_1+\vec{r}_2)/2)}{\rho_0}\right)^{\gamma}\right]\delta(\vec{r}_1 - \vec{r}_2) \quad (2)$$

is employed, where $\vec{r}_1$ and $\vec{r}_2$ are the spatial coordinates of the paired nucleons, ρ is the total density, $\rho_0 = 0.16$ fm^{-3}, and $\gamma = 1$ for the sake of simplicity. We have chosen $\eta = 1$ (surface pairing), and the value of V_0 has been determined by requiring the reasonable reproduction of the pairing gaps along the Ni isotopic chain, focusing, in particular, on the values obtained in ^{64,66}Ni. It is found that $V_0 = 680$ and 760 MeV for the case of SkX and SLy5, respectively.

The results of the calculations for ^{66}Ni are reported in the top part of Table I. We find that the B(E3) values are of the order of 8 W.u. This value can be considered reasonable, in view of the fact that the same kind of calculation for ^{64}Ni provides rather similar results (9.1 and 9.8 W.u. in the case of SkX and SLy5, respectively) and these are just slightly smaller than the weighted average of the experimental measurements for this nucleus [30].

PVC calculations were then performed for the $\pi(2p_{3/2}) \otimes 3^-$ multiplet of ^{67}Cu. These calculations have been improved compared to the previous studies of ^{47,49}Ca, since, in addition to lowest order corrections to the energy of the states, we now include lowest order corrections to the B(E3) as well (cf. the detailed formulas reported in Ref. [24]). The latter corrections tend to reduce the collectivity of the coupled states. Table I lists the results for the $9/2^+$ state of ^{67}Cu. Thus, it is found that the calculated B(E3) value is smaller than the present experimental value. ^{67}Cu deserves further theoretical investigation by considering other coupling modes not included in the present calculation.

B. Shell-model calculations

Single- and few-particle excitations reveal the rigidity of the $Z = 28$ closed shell and shell structure around this region. Nuclei in the neutron-rich Ni region still represent a challenge to modern shell-model calculations owing to the need for a huge diagonalization space required to account for the collective effects [11].

Shell-model calculations for Cu isotopes within the restricted $f_{5/2}p_{3/2}p_{1/2}g_{9/2}$ model space were recently performed [11,31]. For this valence space, the jj44b effective interaction [11,31,32] proved able to reproduce the onset of collectivity above $N = 40$ [31] and to correctly predict the ordering and the excitation energy of the low-lying negative-parity states in ^{67}Cu [11]. In Ref. [31] properties like excitation energies, magnetic moments, and quadrupole moments were compared to experimental values for Cu isotopes with N from 28 to 46, while in Ref. [11] a detailed comparison with energy levels of ^{65,67}Cu was performed. But only the low-lying negative-parity states were considered. From the study of ^{65,67}Cu [11] it is concluded that the positive-parity states are somewhat better described (as excitation energies) by a weak coupling of a $p_{3/2}$ proton to the negative-parity states of the ^{64,66}Ni cores than by the shell-model calculations. It is thus very interesting to investigate how the shell-model calculations describe the structure and decay of the $9/2^+$ state in ^{67}Cu.

We performed calculations with the NUSHELLX@MSU code [33,34] using the jj44b interaction. The calculated excitation energies of the lowest excited states ($5/2^-_1$, 1115 keV; $7/2^-_1$, 1669 keV; $9/2^+_1$, 2503 keV; $13/2^+_1$, 3364 keV) reproduce those given in Ref. [11]. In general, as observed by Chiara *et al.* [11] the predicted spectrum is somewhat more compressed in energy, the calculated states being lower by roughly 300 keV than the experimental ones.

The $3/2^-$ ground state is predicted to have a single-particle character, with a large component of 89% given by the $p_{3/2}$ proton coupled to a neutron configuration of spin 0. The $9/2^+$ state has a more mixed calculated structure, dominated by two components: $\sim$32% $|(\pi g_{9/2})^1 \otimes J_\nu = 0^+\rangle$ and $\sim$39% $|(\pi p_{3/2})^1 \otimes J_\nu = 3^-\rangle$. This composition of the wave function indicates an important single-particle character of this level, as suggested by the experimental spectroscopic factors determined in transfer reactions. The second component points towards the idea of a collective character of the wave function. This result was also expected considering the large experimental B(E3) value suggested [3] for the $9/2^+$ state in ^{67}Cu. Actually, the neutron configurations of the two dominant components of the $9/2^+$ state are very similar to those calculated for the $0^+_{\text{g.s.}}$ and 3^-_1 states of ^{66}Ni.

The E3 transition strength obtained using "standard" effective charges $e_\pi = 1.5e$ and $e_\nu = 0.5e$ is equal to 8.58 W.u., a value that differs from the experimental value by a factor of about 2. Renormalization of the effective charges to $e_\pi = 1.5e$ and $e_\nu = 1.1e$ was proposed by Vingerhoets *et al.* [31] in order to reproduce electric quadrupole moments and magnetic dipole moments for the ground states and some excited states in Cu isotopes with $A = 57$–79. This renormalization compensates for the polarization effect induced by the use of a too restricted valence space, which does not allow excitations of $1f_{7/2}$ proton. With the latter effective charges, the resulting B(E3) becomes 17.95 W.u., which compares better with the experimental value. Nevertheless, this result has to be considered with care, since the effective charges for octupole excitations *a priori* do not necessarily agree with those used in the description of quadrupole excitations.

TABLE II. Comparison between calculated (present work) and experimental proton pickup spectroscopic strengths.

	$(2j+1)C^2S_{lj}$	
	Shell-model calculation	^{68}Zn(d,^{3}He)^{67}Cu [7]
$3/2^-$	0.91	1.9
$5/2^-$	0.54	0.30
$1/2^-$	0.24	0.26
$9/2^+$	0.14	—

Further tests of the shell-model wave functions were made by comparing calculated and experimental spectroscopic factors for one-proton transfer reactions. Direct information of this type for the ^{67}Cu nucleus exists only for the (d,^{3}He) pickup reaction [7]. Table II reports this comparison, and it can be seen that, with the exception of a factor of about 2 for the $3/2^-$ ground state, there is reasonably good agreement for the $5/2^-_1$ and $1/2^-_1$ states. The spectroscopic factor for the $7/2^-_1$ state could not be calculated due to the unavailability of the $1f_{7/2}$ orbital in the adopted model space, while the experimental spectroscopic factor for the $9/2^+$ state is unfortunately missing.

^{67}Cu cannot be reached by one-proton stripping reactions. Nevertheless, indirect information on this process can be obtained from the experimental data on the (α,p) reaction [10]. By normalizing the angular distributions calculated using the DWBA formalism with a cluster form factor, transition strengths could be determined for the low-lying excited states. These relative transition strengths (i.e., normalized to that of the $3/2^-$ ground state) in the case of the ^{64}Ni(α,p)^{67}Cu reaction were observed to be similar to those of the ^{62}Ni(α,p)^{65}Cu reaction [10]. Furthermore, the relative transition strengths for ^{65}Cu were observed to be practically equal to the relative values of the $(2j+1)C^2S_{lj}$ quantities in the one-proton stripping reactions (^{3}He,d) and (α,t), due to the role of spectator played by the transferred pair of neutrons in the (α,p) reaction [10]. With these two facts in mind, we compare in Table III the calculated relative one-proton transfer strengths to ^{66}Ni (unstable nucleus) with the relative strengths observed in the ^{62}Ni(α,p)^{65}Cu reaction [10]. Again, we observe a reasonable agreement, the largest discrepancy, of a factor of about 2, being for the $5/2^-_1$ state.

In view of the discrepancies of up to a factor of 2 reported in both Table II and Table III, one can state that there is qualitative agreement between the predicted shell-model spectroscopic factors and the trend of the experimental values.

The M2 branch (1387.2 keV) of the decay of the $9/2^+$ state has been calculated as $B(\text{M2};\ 9/2^+ \rightarrow 5/2^-) = 2.098$ W.u. [using standard (bare nucleon) proton and neutron gyromagnetic factors], compared to the experimental value of

TABLE III. Calculated relative $(2j+1)C^2S_{lj}$ values for a proton stripping reaction on ^{66}Ni as a target and relative spectroscopic strengths from the three-nucleon transfer reaction (α,p). The latter are not available for the ^{64}Ni$(\alpha,p)^{67}$Cu reaction, but according to Ref. [10], they are similar to those for the ^{62}Ni$(\alpha,p)^{65}$Cu reaction (see also the text).

	Relative spectroscopic strength	
	Shell-model calculation	^{62}Ni$(\alpha,p)^{65}$Cu [10]
$3/2^-$	1	1
$5/2^-$	1.09	0.44
$1/2^-$	0.31	0.40
$9/2^+$	1.21	0.85

0.146(15) W.u. The difference between the calculated and the measured value may be due to the too restricted configuration space. Indeed, calculations in odd-mass nuclei around ^{208}Pb indicated that the B(M2) values are extremely sensitive to the dimensions of the configuration space [35]. The need to allow for proton excitations across $Z = 28$ (thus including the $1f_{7/2}$ orbital) in order to account for the nuclear structure evolution observed in the odd Cu isotopes with $N = 40$–50 was also emphasized by Sieja and Nowacki [36]. This seems to be the case for neutron-rich Cu isotopes and therefore the core polarization induced by proton particle-hole excitations has to be included in the effective charges.

The M1 transition between the $15/2^+$ and the $13/2^+$ states was calculated using bare nucleon values for gyromagnetic factors. The shell model predicts dominant configurations of $[\pi(p_{3/2})\nu(f^3_{5/2}p^4_{3/2}p^2_{1/2}g^1_{9/2})]_{15/2^+}$ and $[\pi(p_{3/2})\nu(f^4_{5/2}p^4_{3/2}p^1_{1/2}g^1_{9/2})]_{13/2^+}$, respectively, for these two states, which do not allow an M1 transition. Nevertheless, the M1 transition may proceed through minor components in the structure of the two states, which explains the observed hindrance for this transition. The calculated strength of $B(\mathrm{M1}; 15/2^+ \to 13/2^+) = 0.0288$ W.u. compares reasonably well with the experimental value of 0.0218(29) W.u.

The B(E2) value for $13/2^+ \to 9/2^+$ calculated using the standard effective charges and considering that this transition is a pure E2 is equal to 0.03 W.u., which is in reasonable agreement with the experimental value of 0.08(1) W.u. The shell-model wave function of the initial state is similar to the wave function of the lowest 5^- state of the ^{66}Ni core, and therefore this transition can be considered as being made by the neutrons, with the proton as a spectator. The E2 reduced transition probability for the $5^- \to 3^-$ transition in ^{66}Ni was measured by Broda *et al.* [17] as 2(1) W.u. The much lower B(E2) value found in ^{67}Cu is a consequence of the fragmented wave function of the $9/2^+$ state, which consists of about a 39% contribution given by the coupling of the $p_{3/2}$ proton with neutron configurations coupled to total spin $J = 3$, while the structure of the $13/2^+$ state is mainly (∼80%) given by the $(\pi p_{3/2})^1 \otimes J_\nu = 5^-$ configuration.

V. CONCLUSIONS

The lifetimes of the yrast $9/2^+$, $13/2^+$, and $15/2^+$ states in ^{67}Cu were measured by using the fast-timing technique. In addition to the $15/2^+$ state proposed [3] as an isomer with a lifetime in the nanosecond range, the $13/2^+$ state has also been found to be an isomer with a similar lifetime.

The measured transition strength of the E3 decay of the $9/2^+$ state indicates an important collective character. In order to understand the measured electromagnetic decay strengths, calculations were made with two structure models: the PVC model and the shell model.

The PVC model within the weak-coupling limit predicts a too low $B(\mathrm{E3}; 9/2^+ \to 3/2^-_{\mathrm{g.s.}})$ value, indicating a collectivity not too far from that of the 3^- of the core nucleus, although somewhat quenched. The shell-model calculations in the restricted $f_{5/2}p_{3/2}p_{1/2}g_{9/2}$ space reproduce better the experimental B(E3) value, especially when a nonstandard value is used for the neutron effective charge. The other measured electromagnetic transition probabilities are in reasonably good agreement with those predicted by the shell-model calculations, especially the strongly hindered E2, $13/2^+ \to 9/2^+$, and M1, $15/2^+ \to 13/2^+$, transitions, respectively. It is expected that the description of the experimental data will improve with the inclusion of the $1f_{7/2}$ orbital in the shell-model space.

ACKNOWLEDGMENTS

The help of C. Petrone (IFIN-HH) in performing the shell-model calculations is greatly appreciated. C.R.N. acknowledges the financial support offered through Contract POSDRU/107/1.5/S/76813. This work was supported through Romanian UEFISCDI Contract PN-II-ID-PCE-2011-3-0367 and by the Istituto Nazionale di Fisica Nucleare (INFN) and the Science and Technology Facilities Council (STFC).

[1] F. Recchia *et al.*, Phys. Rev. C **85**, 064305 (2012).
[2] I. Ştefănescu *et al.*, Phys. Rev. Lett. **100**, 112502 (2008).
[3] M. Asai, T. Ishii, A. Makishima, I. Hossain, M. Ogawa, and S. Ichikawa, Phys. Rev. C **62**, 054313 (2000).
[4] A. M. Oros-Peusquens and P. F. Mantica, Nucl. Phys. A **669**, 81 (2000).
[5] R. M. Britton and D. L. Watson, Nucl. Phys. A **272**, 91 (1976).
[6] A. G. Blair, Phys. Rev. **140**, B648 (1965).
[7] B. Zeidman and J. A. Nolen, Phys. Rev. C **18**, 2122 (1978).
[8] P. Roussel, G. Bruge, A. Bussiere, H. Faraggi, and J. E. Testoni, Nucl. Phys. A **155**, 306 (1970).
[9] D. Bachner, R. Bock, H. H. Duhm, R. Santo, and R. Stock, Nucl. Phys. A **99**, 487 (1967).
[10] D. Bucurescu, M. Ivaşcu, G. Semenescu, and M. Titirici, Nucl. Phys. A **189**, 577 (1972).
[11] C. J. Chiara *et al.*, Phys. Rev. C **85**, 024309 (2012).

[12] A. L. McCarthy and G. M. Crawley, Phys. Rev. **150**, 935 (1966).
[13] J. Huo, X. Huang, and J. K. Tuli, Nucl. Data Sheets **106**, 159 (2005). Data retrieved from the ENSDF database, http://www.nndc.bnl.gov/ensdf.
[14] E. Runte, K.-L. Gippert, W.-D. Schmidt-Ott, P. Tidemand-Petersson, L. Ziegeler, R. Kirchner, O. Klepper, P. O. Larsson, E. Roeckl, D. Schardt, N. Kaffrell, P. Peuser, M. Bernas, P. Dessagne, and M. Langevin, Nucl. Phys. A **441**, 237 (1985).
[15] K. Nybø, H. Helstrup, T. F. Thorsteinsen, and G. Løvhøiden, Phys. Scripta **63**, 181 (2001).
[16] J. H. Bjerregaard and O. Nathan, Nucl. Phys. **85**, 593 (1966).
[17] R. Broda, T. Pawlat, W. Krolas, R. V. F. Janssens, S. Zhu, W. B. Walters, B. Fornal, C. J. Chiara, M. P. Carpenter, N. Hoteling, L. W. Iskra, F. G. Kondev, T. Lauritsen, D. Seweryniak, I. Stefanescu, X. Wang, and J. Wrzesinski, Phys. Rev. C **86**, 064312 (2012).
[18] H. Mach, R. L. Gill, and M. Moszynski, Nucl. Instrum. Meth. A **280**, 49 (1989).
[19] M. Moszynski and H. Mach, Nucl. Instrum. Meth. A **277**, 407 (1989).
[20] N. Mărginean, D. L. Balabanski, D. Bucurescu, S. Lalkovski, L. Atanasova, G. Căta-Danil, I. Căta-Danil, J. M. Daugas, D. Deleanu, P. Detistov, G. Deyanova, D. Filipescu, G. Georgiev, D. Ghiţă, K. A. Gladnishki, R. Lozeva, T. Glodariu, M. Ivaşcu, S. Kisyov, C. Mihai, R. Mărginean, A. Negret, S. Pascu, D. Radulov, T. Sava, L. Stroe, G. Suliman, and N. V. Zamfir, Eur. Phys. J. A **46**, 329 (2010).
[21] T. Ishii, M. Asai, A. Makishima, I. Hossain, M. Ogawa, J. Hasegawa, M. Matsuda, and S. Ichikawa, Phys. Rev. Lett. **84**, 39 (2000).
[22] C. D. Nesaraja, Nuclear Data Sheets **115**, 1 (2014).
[23] A. Bohr and B. R. Mottelson, *Nuclear Structure*, 1st and 2nd eds. [W. A. Benjamin (Open Library), 1975]; https://openlibrary.org/works/OL9400115W/Nuclear_Structure.
[24] I. Hamamoto, Phys. Rep. **10**, 63 (1974).
[25] D. Montanari *et al.*, Phys. Lett. B **697**, 288 (2011).
[26] D. Montanari *et al.*, Phys. Rev. C **85**, 044301 (2012).
[27] G. Coló, P. F. Bortignon, S. Fracasso, and N. Van Giai, Nucl. Phys. A **788**, 137c (2007).
[28] B. A. Brown, Phys. Rev. C **58**, 220 (1998).
[29] E. Chabanat, P. Bonche, P. Haensel, J. Meyer, and R. Schaeffer, Nucl. Phys. A **643**, 441 (1998).
[30] T. Kibedi and R. H. Spear, At. Data Nuclear Data Tables **80**, 35 (2002).
[31] P. Vingerhoets, K. T. Flanagan, M. Avgoulea, J. Billowes, M. L. Bissell, K. Blaum, B. A. Brown, B. Cheal, M. De Rydt, D. H. Forest, Ch. Geppert, M. Honma, M. Kowalska, J. Krämer, A. Krieger, E. Mané, R. Neugart, G. Neyens, W. Nörtershäuser, T. Otsuka, M. Schug, H. H. Stroke, G. Tungate, and D. T. Yordanov, Phys. Rev. C **82**, 064311 (2010).
[32] B. A. Brown and A. F. Lisetskiy (unpublished).
[33] B. A. Brown, W. D. M. Rae, E. McDonald, and M. Horoi, http://www.nscl.msu.edu/brown/resources/resources.html.
[34] W. D. M. Rae, http://www.garsington.eclipse.co.uk/.
[35] R. Bauer, J. Speth, V. Klemt, P. Ring, E. Werner, and T. Yamazaki, Nucl. Phys. A **209**, 535 (1973).
[36] K. Sieja and F. Nowacki, Phys. Rev. C **81**, 061303(R) (2010).